Catalysis Today 141 (2009) 245–253

Contents lists available at ScienceDirect

Catalysis Today

journal homepage: www.elsevier.com/locate/cattod

Propane oxidative dehydrogenation over vanadia catalysts supported on mesoporous silicas with varying pore structure and size

S.A. Karakoulia [a,d], K.S. Triantafyllidis [b,**], G. Tsilomelekis [c], S. Boghosian [c], A.A. Lemonidou [a,d,*]

[a] Department of Chemical Engineering, Aristotle University of Thessaloniki, P.O. Box 1517, University City, Thessaloniki 54124, Greece
[b] Department of Chemistry, Aristotle University of Thessaloniki, P.O. Box 116, University City, Thessaloniki 54124, Greece
[c] Department of Chemical Engineering, University of Patras and FORTH/ICE-HT, Patras 26500, Greece
[d] Chemical Process Engineering Research Institute, CERTH, P.O. Box 60361 Thermi, Thessaloniki 57001, Greece

ARTICLE INFO

Article history:
Available online 9 July 2008

Keywords:
Mesoporous silicas
Oxidative dehydrogenation
Propane
Propene
Vanadia

ABSTRACT

The structural characteristics and the performance of vanadia catalysts (0.7–8 wt.% V) supported on mesoporous (MCM-41, HMS, MCF, SBA-15), microporous (silicalite) and non-porous (SiO_2) silicas in oxidative dehydrogenation of propane were investigated. The structure of vanadia species, the redox and the acidic properties of the catalysts were studied using *in situ* Raman spectroscopy, TPD- NH_3 and H_2-TPR. The only vanadia species detected on the surface of HMS and MCM-41 for V loadings up to 8 wt.% were isolated monovanadates indicating high vanadia dispersion. Additional bands ascribed to V_2O_5 nanoparticles were evidenced in the case of SBA-15 and MCF supported catalysts while these bands were the only ones identified on the surface of the catalysts supported on silicalite and non-porous silica. The catalysts supported on mesoporous HMS and MCM-41 materials showed the best performance achieving high propane conversions (35–40%) with relatively high propene selectivities (35–47%). Lower activity due to the lower degree of vanadia dispersion, caused by the partial destruction of the pore structure was observed for the SBA-15 and MCF supported catalysts. The degree of dispersion of the V species on the catalyst surface and not the pore size and structure of the mesoporous support or the acidity/reducibility characteristics mainly determine the catalytic activity towards propene production. In addition, it was shown that the pore structure and size of the mesoporous supports did not have any significant effect in the turnover rates (TOF values) of propane conversion (and propene formation at low propane conversion, below ca. 10%). However, the highest propene yield (up to 19%) and stable catalytic behavior was attained for catalysts supported on HMS mesoporous silica, and especially for those combining framework mesoporosity and textural porosity (voids between primary nanoparticles).

1. Introduction

The increased demand for propene has spurred the interest for the development of new selective reaction routes overcoming the drawbacks of the established industrial processes. Oxidative dehydrogenation (ODH) of propane is an attractive alternative for propene production as the presence of oxygen raises the thermodynamic restrictions of dehydrogenation and the exothermic character of the reaction renders it an energetically efficient process [1]. The challenge in this reaction is the development of a catalyst able to activate the C–H bond at relatively low temperatures while hindering the undesirable oxidation reaction of propene to CO_x products [2,3]. Vanadia supported catalysts have been proven so far as ones of the most active and selective catalysts in this reaction [1–5]. High selectivity to propene is favored by the presense of monomeric or even oligomeric tetrahedral V^{5+} species; the O atom bridging V to the support has been suggested to activate propane [6,7]. The composition of the support influences the speciation of VO_x species into monovanadates, polyvanadates and V_2O_5 clusters and thus the catalytic behavior of supported vanadia in ODH reactions [8]. Silica supported vanadia catalysts are reported as highly selective towards propene production because they do not favor consequent combustion reactions to CO_x species, compared to other more acidic supports, such as alumina and titania [9,10].

High surface area mesoporous silica supports, such as M41S [11–14], HMS [15,16], SBA-15 [17,18] and MCF [19], have shown promising catalytic performance in the ODH of propane mainly

* Corresponding author. Tel.: +30 2310 996273; fax: +30 2310 996184.
** Corresponding author. Tel.: +30 2310 997730; fax: +30 2310 997730.
E-mail addresses: ktrianta@chem.auth.gr (K.S. Triantafyllidis), alemonidou@cheng.auth.gr (A.A. Lemonidou).

0920-5861/$ – see front matter © 2008 Elsevier B.V. All rights reserved.
doi:10.1016/j.cattod.2008.05.024

due to the high degree of vanadia dispersion. The dependence of catalytic performance on vanadia dispersion is of great importance. Kondratenko et al. [11] investigated the effect of vanadium loading on the formation of vanadia crystalline phases on MCM-41 material synthesized either by addition of vanadium source (vanadyl sulfate) during MCM-41 synthesis or by impregnation of MCM-41 with vanadium acetyl acetate in toluene. In both cases, no crystalline V_2O_5 phases were identified for vanadium loading up to 5.3 wt.% while intense XRD reflections corresponding to V_2O_5 crystals were determined for higher vanadium loading (11.2 wt.%). The presence of V_2O_5 crystals (for loadings higher than 5.3 wt.%) induced a significant decrease in selectivity (from 70% to 20%) even for relatively low propane conversions (4–6%). Zhou et al. [15] did not observe any diffraction features corresponding to V_2O_5 crystals even for vanadium loadings up to ~17 wt.% for the HMS based catalysts. However, in the same work, Raman measurements showed that when vanadium content was above 5.6 wt.% the characteristic bands of V_2O_5 crystals could be detected. The maximum propene yield of 13.9% was obtained over the supported vanadia catalyst with 5.6 wt.% V while for samples with higher V loadings there was a rapid decrease in propene selectivity especially at high propane conversions. Liu et al. [17] observed that most vanadium cations are tetrahedrally coordinated on the surface of SBA-15 for V loadings up to 4.5 wt.%, while a crystalline V_2O_5-phase begins to appear at higher loadings. The catalyst with the best performance in the ODH of propane was the 2.8 wt.% V supported on SBA-15. The same group showed that for V loadings up to 4.2 wt.% on MCF (foam-like silica) no vanadia crystals were formed based on Raman measurements; this catalyst sample provided also the highest propene yield [19].

In our previous work [20], we have shown that impregnation of SBA-15 and MCF mesoporous silicas with vanadium oxalate (derived from dissolution of NH_4VO_3 in oxalic acid aqueous solutions) resulted in a partial breakdown of the mesoporous structure, leading to relatively lower dispersion of vanadia species compared to the respective MCM-41 and HMS supported catalysts. Preliminary screening of the above mentioned samples showed that the SBA-15 and MCF supported catalysts were less active than the MCM-41 and HMS supported catalysts. The aim of the present work is to investigate further the difference in the catalytic performance of the various mesoporous silica supported catalysts in the ODH of propane by examining their structural and surface characteristics. Catalytic measurements are complemented with *in situ* Raman, H_2-TPR and NH_3-TPD studies. A comparison with vanadia catalysts supported on microporous zeolite silicalite and non-porous silica is also reported.

2. Experimental

2.1. Preparation of supported vanadia catalysts

The supported vanadia catalysts were prepared by wet impregnation of the silica supports using NH_4VO_3 (Merck) dissolved in aqueous solution of oxalic acid (molar ratio NH_4VO_3/oxalic acid = 1/2). The vanadium loading was varied in order to achieve 0.7–8 wt.% V in the final calcined catalysts. More experimental details on the preparation of the catalysts are given in our previous work [20]. The silica supports used were various mesoporous silicas (MCM-41, HMS, SBA-15 and MCF) synthesized in our laboratory as well as the microporous zeolite silicalite (UOP) and a non-porous silica (Sigma–Aldrich). All catalysts, after impregnation, were dried at room temperature for at least 24 h followed by drying at 100 °C for 3 h, and then calcined at 500 °C in air flow for 4 h. The catalytic samples were named as *x*V-*support*, were *x* is the weight percentage of vanadium in the catalyst and *support* is the type of the support used.

2.2. Characterization of vanadia catalysts

N_2 adsorption–desorption experiments at −196 °C were performed on an Automatic Volumetric Sorption Analyzer (Autosorb-1, Quantachrome) for the determination of surface area (BET method), pore volume and pore size distribution (BJH method) of the samples that were previously outgassed at 150 °C for 16 h under vacuum (1.33×10^{-1} Pa).

The types of the V species formed on the surface of the siliceous supports were studied with *in situ* Raman spectroscopy. Approximately 180 mg of each catalyst were pressed into a wafer and mounted on a holder that could be adjusted in the vertical core of the *in situ* Raman cell, which is described elsewhere [21]. The 514.5-nm line of a Spectra Physics Stabilite 2017 Ar^+ laser operated at 30 mw on the sample was used for recording of the Raman spectra. The laser beam was focused on the sample with a cylindrical lens in order to reduce sample irradiance. The scattered light was collected at 90°, analyzed with a 0.85 m Spex 1403 double monochromator and detected by a −20 °C cooled RCA PMT equipped with EG&G photon counting electronics. Recording of spectra was performed at 430 °C under flowing O_2 after the sample was exposed for 1 h at 430 °C in flowing O_2.

The reducibility and the acidic characteristics of the vanadia catalysts were studied with temperature programmed reduction with H_2 (TPR-H_2) and NH_3-temperature programmed desorption (TPD-NH_3), respectively. In a typical experiment, 0.2 g of the sample were loaded in a U-shaped quartz reactor and pre-treated at 500 °C in He for 0.5 h. In the case of H_2-TPR experiment, the catalyst was cooled to 40 °C and then the temperature was increased from 40 to 800 °C at a heating rate of 10 °C/min in a 5% H_2/He flow rate of 30 ml/min. The composition of the exit gas was monitored on-line by a quadrupole mass analyzer (Omnistar, Balzers). The main *m/z* fragments registered were H_2 = 2, H_2O = 18, He = 4. In a typical TPD-NH_3 experiment, the catalyst was cooled to 100 °C (after pretreatment at 500 °C) under He flow and then treated with a flow of 5% NH_3/He for 1 h at 100 °C. Flushing with pure helium at 100 °C for 2 h was then applied to remove the physisorbed ammonia. TPD analysis was carried out from 100 to 800 °C at a heating rate of 10 °C/min and a helium flow rate of 30 ml/min. The *m/z* fragments registered were as follows: NH_3 = 17, 16, 15, H_2O = 18, N_2 = 28, NO = 30, N_2O = 44. Quantitative analysis of the desorbed ammonia was based on *m/z* = 15.

2.3. Catalytic tests

Catalytic experiments of the propane ODH were conducted in a fixed bed quartz reactor (9 mm i.d., 300 mm length) equipped with coaxial thermocouple. The catalyst powders were pressed, crushed and sieved to average particle size of 20–100 μm. The catalyst was loaded to the reactor after mixing with equal amounts of quartz beads. Prior to testing, the catalyst was treated in oxygen flow (10% O_2 in He) at 450 °C for 30 min. The composition of the reacting mixture used was C_3H_8/O_2/He = 5/5/95. The catalytic performance was tested as a function of the reaction temperature ranging from 425 to 600 °C using the same catalyst weight (W = 0.2 g) and total flow rate (F = 105 cm^3 min^{-1}). In addition, tests with variable W/F at 550 °C were performed. The products were analyzed on line using a PerkinElmer Autosystem XL gas chromatograph equipped with a thermal conductivity detector (TCD) [20]. The propane conversion and the selectivity of the products were calculated on a carbon basis.

3. Results and discussion

3.1. Physicochemical characteristics of supported vanadia catalysts

Detailed characterization data of the structure and porosity of the synthesized mesoporous silicas used as supports in this study are provided in our previous publication [20]. The well-ordered hexagonal pore structure of the mesoporous MCM-41 and SBA-15 as well as the disordered wormhole-like pore structure of HMS and the mesocellular foam-like structure of MCF supports were verified with XRD measurements in the 2θ range of 0.5–10° and TEM images. The N_2 adsorption–desorption experiments revealed high surface areas (770–970 m^2/g) and uniform pore sizes (in the range of 2.3–20 nm) for all the synthesized mesoporous silicas. In the case of HMS mesoporous silica, the synthesis route was modified in order to obtain additional textural porosity (interparticle voids). Sample HMS-1 contains only framework mesoporosity while samples HMS-2 and 3 contain additional textural porosity [20].

Table 1 presents composition and porosity characteristics of the vanadia catalysts supported on the non-porous (SiO_2), the microporous (silicalite) and the mesoporous silicas (MCM-41, HMS-1,2,3, SBA-15 and MCF). Wet impregnation of the mesoporous silica samples with vanadium oxalate complex under relatively strong acidic conditions (pH 2) resulted in a decrease of surface area of the supported catalysts, which was more intense at higher V loadings. This decrease was more drastic in the case of SBA-15 and MCF supported catalysts, being attributed to a partial destruction of the framework mesoporous structure as evidenced by TEM images [20]. The surface area loss ranged from ca. 5% for the 2V-HMS-2 sample to 53% for the 8V-SBA-15 sample (Table 1). However, all the vanadia catalysts on mesoporous supports exhibited high surface areas (from ca. 420 to 930 m^2/g).

The surface structure of the supported vanadia catalysts and the type of vanadia species was studied by *in situ* Raman spectroscopy at 430 °C under O_2. Representative spectra are shown in Fig. 1 and correspond to the fully oxidised state of the catalysts under dehydrated conditions. For catalysts supported on mesoporous HMS and MCM-41 (with VO_x surface densities, n_s, in the range of 0.09–1.33 V/nm^2) the predominant surface V species appear to be the isolated monovanadates with one terminal V=O (observed at 1038–1040 cm^{-1}, Fig. 1a) and three V–O–Si anchoring bonds in a C_{3v}-like configuration with tetracoordinated vanadium [22]. In the case of the catalyst with the highest V loading (8V–HMS–2 with n_s = 1.33 V/nm^2) a small peak at ~997 cm^{-1} indicates the existence of traces of bulk V_2O_5 nanoparticles. The band at around ~975 cm^{-1}, assigned to Si–OH stretching modes decreases with increasing V loading due to consumption of Si-OH groups by anchoring VO_x species [23]. The bands observed at ~480 cm^{-1} and ~610 cm^{-1} are due to defect modes attributed to tri- and tetracyclosiloxane rings produced via condensation of surface hydroxyls [24]. The above silica vibrations are much weaker for the respective pure siliceous support (Fig. 1) due to the low polarizability of light atoms and the ionic character of the Si–O bonds [25]. The dispersion and consequently the type (monovanadates or bulk crystalline vanadia) of vanadium species on the surface of the support depends both on the V loading and the surface area of the support. A vanadium surface density of 0.7 V atoms/nm^2 has been reported as the maximum monolayer coverage for a silica support with a medium surface area (~300 m^2/g) [26]. When a high surface area MCM-41 mesoporous silica was impregnated with vanadium acetyl acetate in toluene, no Raman bands attributed to V_2O_5 were observed for n_s values as high as 0.8 V/nm^2 [11]. In the present work, no crystalline V_2O_5 has been detected for the V-HMS and V-MCM-41 samples with surface densities up to ~1.3 V/nm^2 (Table 1), indicating the accommodation of higher amount of monovanadate species on the silica surface.

The Raman spectra of 4V-MCF and 4V-SBA-15 catalysts (with n_s of 1.83 and 0.81 V/nm^2) exhibited the characteristic bands due to crystalline V_2O_5 (at 996 and 282 cm^{-1}, see Fig. 1b). Nevertheless, judged from the intensity of the 1038 cm^{-1} V=O band of the isolated monovanadates for 4V-MCF and 4V-SBA-15 as compared

Table 1
Composition and porosity characteristics of supported vanadia catalysts

Catalyst	Vanadium loading[a] (wt.%)	VO_x surface density, n_s (VO_x/nm^2)	Surface area[b] (m^2/g)	Surface area loss[c] (%)	Total pore volume at P/P_o = 0.99 (cm^3/g)	Average pore diameter[d] (nm)
0.7V-MCM-41	1.1	0.15	746	21	0.73	2.66
2V-MCM-41	1.7	0.23	863	9	0.79	2.87
4V-MCM-41	4.6	0.68	801	15	0.70	2.87
8V-MCM-41	7.5	1.30	678	28	0.61	2.70
0.7V-HMS-1	0.7	0.10	775	20	0.67	2.16
2V-HMS-1	2.0	0.31	768	21	0.64	2.15
4V-HMS-1	4.0	0.60	875	18	0.58	2.28
8V-HMS-1	7.8	1.53	599	38	0.47	2.17
1.3V-HMS-2	1.3	0.09	937	1	1.78	2.80
2V-HMS-2	2.2	0.29	899	5	1.59	2.70
4V-HMS-2	4.3	0.60	788	10	1.51	2.28
8V-HMS-2	7.9	1.33	705	26	1.25	2.71
2V-HMS-3	2.3	0.39	694	10	1.05	3.28
4V-HMS-3	4.4	0.78	668	13	0.98	3.29
8V-HMS-3	8.1	1.75	546	29	0.84	3.14
4V-SBA-15	4.2	0.81	611	31	0.70	6.65
8V-SBA-15	7.9	2.25	417	53	0.56	6.47
4V-MCF	4.6	1.83	444	46	0.61	19.5
2V-silicalite	2.5	0.82	359	6	0.23	~0.55
4V-silicalite	4.2	1.62	325	15	0.23	~0.55
8V-silicalite	8.2	3.11	311	18	0.20	~0.55
2V-SiO_2	2.4	32.8	8.8	n.d.	0.60	n.d.
4V-SiO_2	4.8	71.4	4.5	n.d.	0.05	n.d.

[a] Obtained by chemical analysis of calcined catalysts with ICP-AES.
[b] Multi-point BET method.
[c] Percentage of surface area loss compared to parent silica support.
[d] Determined by BJH method from N_2 adsorption data.

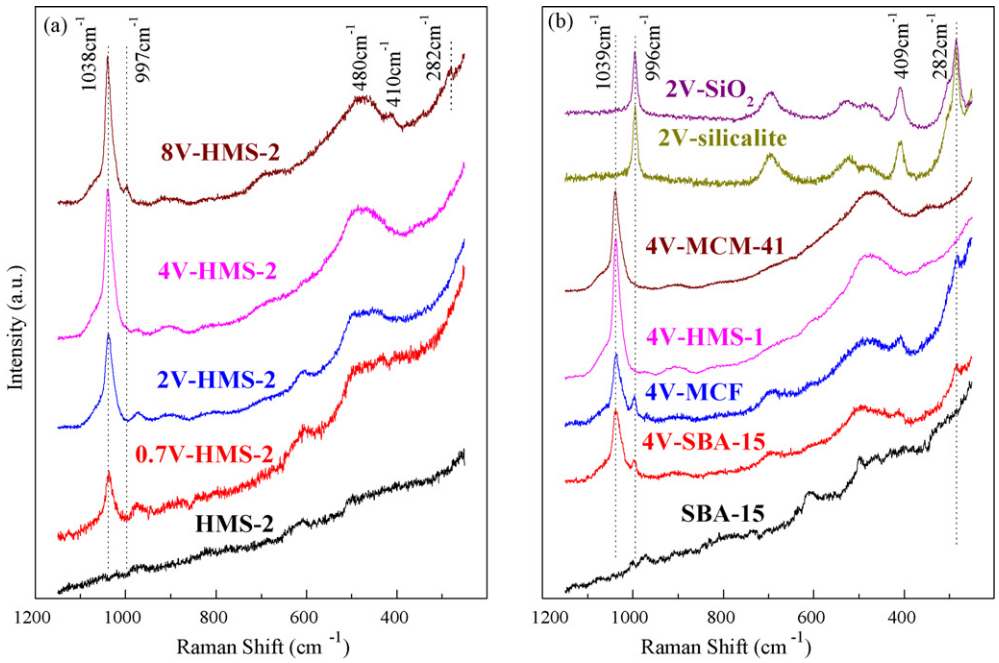

Fig. 1. *In situ* Raman spectra obtained at 430 °C under O_2 atmosphere for vanadia catalysts supported on (a) HMS-2 mesoporous silica and (b) various mesoporous (MCM-41, HMS-1, MCF, SBA-15) silicas, microporous silicalite and non-porous SiO_2 samples with different V loadings.

to the intensity of the 997 cm^{-1}–V_2O_5 band, it turns out that the isolated monovanadates are again the dominant surface species for these two catalyst samples. This conclusion is further strengthened by taking into account the 10-fold scattering cross-section of the bulk species compared to the amorphous isolated vanadate [27]. It is to be noted that these bulk V_2O_5 particles are XRD-silent for these two samples [20], indicating that their size is particularly small (less than 4 nm). Previous Raman studies of vanadia supported on SBA-15 substrates showed no crystalline V_2O_5 features for surface densities up to 1.45 V/nm^2 [28] or 0.69 V/nm^2 [17]. Furthermore, a previous study on MCF based catalysts claimed the existence of both isolated and polymeric vanadates for n_s up to 1.08 V/nm^2, while bands due to V_2O_5 crystals appeared for n_s above 1.61 V/nm^2 [18]. However, in agreement with the findings of the present work, formation of associated (polymeric) surface vanadates is known not to occur on silica substrates under dehydrated conditions [8,24]. The relatively weak interaction of silica with vanadia leads either to monomeric isolated vanadates or to bulk vanadia crystals depending on the V loading.

In the case of silicalite and SiO_2 based catalysts shown in Fig. 1b (with n_s of 0.8 and 32.8 V/nm^2), the only bands detected are due to bulk V_2O_5 (997, 696, 522, 409, 282 cm^{-1}). No features due to V isolated species are observed for these samples. The absence of monomeric species particularly in the case of silicalite can be ascribed to the acid character of the support which favors agglomeration of VO_x units to form V_2O_5 crystals [29]. In addition, insertion of vanadium in the narrow silicalite channels (diameter ~5.5 Å) in the form of vanadium oxalate complex could be inhibited by its relatively large size (~5 × 8 Å), thus leading to the formation of bulk V_2O_5 crystalline phases on the external surface of the silicalite crystals [20].

The reduction behavior of the vanadium oxide species deposited on the surface of the non-porous, microporous and mesoporous silicas was studied by means of H_2-TPR. Fig. 2a depicts

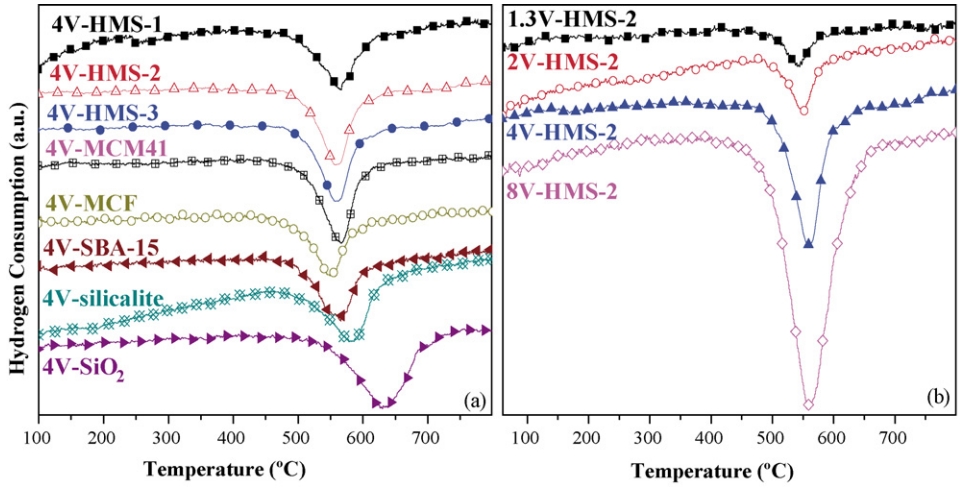

Fig. 2. TPR curves of vanadia catalysts supported on (a) different silicas with 4 wt.% V and (b) mesoporous HMS-2 with various V loadings.

Table 2
Acidic and redox characteristics of supported vanadia catalysts

Catalyst	Total acidity[a] (mmol NH_3/g)	T_{max}[b] (°C)	AOS[c]
4V-MCM-41	0.21	567	3.66
4V-HMS-1	0.21	565	3.69
1.3V-HMS-2	0.07	548	3.41
2V-HMS-2	0.17	551	3.77
4V-HMS-2	0.25	559	3.62
8V-HMS-2	0.41	560	3.45
4V-HMS-3	0.20	548	3.72
4V-SBA-15	0.39	565	3.4
4V-MCF	0.32	550	3.65
4V-silicalite	0.10	585	3.22
4V-SiO_2	~0.01	633	2.89

[a] From TPD-NH_3 experiments.
[b] Temperature of maximum H_2 consumption in TPR-H_2 experiments, see Fig. 2.
[c] AOS = Average vanadium oxidation state calculated from TPR-H_2 results.

the TPR results of vanadia catalysts supported on different silica samples with 4 wt.% V. The TPR profiles for all the catalysts supported on mesoporous silicas show a maximum of hydrogen consumption at about 540–570 °C (Table 2) which is mainly attributed to the reduction of monomeric VO_x (V^{5+}) surface species [30–32]. In the case of microporous silicalite and non-porous SiO_2 based catalysts, there is a shift to higher temperatures which is in accordance with the presense of crystalline V_2O_5 phases (Raman results). The TPR profiles for vanadia catalysts supported on the HMS-2 mesoporous sample with 1.3–8 wt.% V (Fig. 2b, Table 2) show a gradual increase of the consumed hydrogen and a marginal shift of the maximum of hydrogen consumption peak to higher temperatures with increasing V loading.

The average oxidation state of vanadium after the reduction, as calculated from the amount of hydrogen consumed, varies between 2.9 and 3.7 (Table 2). The catalysts supported on non-porous SiO_2 and microporous silicalite, which contain mainly bulk crystalline vanadia, showed an oxidation state of ~3 indicating a full reduction of V^{5+} to V^{3+}. On the other hand, the oxidation state of vanadium for the catalysts supported on mesoporous silicas, which contain mostly monomeric vanadia moities, averages at about 3.5–3.7. This oxidation state can be attributed to incomplete reduction to V^{4+}/V^{3+} and/or to the presence of V^{4+}/V^{3+} species on the surface of the catalysts before the reduction [33]. The direct interaction of monomeric vanadia species with the silica surface (Si-O-V) could be the reason for the inhibition of full reduction of V^{5+} to V^{3+}, compared to complete reduction of the bulk crystalline vanadia on the surface of SiO_2 or silicalite.

The acidic characteristics of the supported vanadia catalysts were studied by NH_3-TPD. The TPD curves are shown in Fig. 3 and the total number of acid sites for the measured catalysts are given in Table 2. All the catalysts supported on mesoporous silicas show one relatively sharp desorption peak at around 200–210 °C related to weak Lewis acid sites which are attributed to isolated vanadium sites tetrahedrally coordinated with oxygen [34,35]. We should mention that no desorption peaks related to acidic sites with medium/high strength were observed (ca. higher than 350 °C) in contrast to other studies concerning vanadia catalysts supported on MCM-41 with similar vanadium loadings [36,37]. The amount of acid sites of the siliceous mesoporous supports was negligible not surpassing ~0.01 mmol NH_3/g (not shown). The number of acid sites increases with increasing vanadium loading, as can be seen for the catalysts with 1.3 to 8 wt.% V on HMS-2 sample (Table 2). When comparing catalysts with the same V loading (4 wt.%) on different mesoporous supports, the SBA-15 and MCF supported catalysts showed a slightly higher number of acid sites compared to the respective MCM-41 and HMS supported catalysts.

The TPD profile of the pure silicalite sample revealed two desorption peaks at 225 and 410 °C (Fig. 3b). The lower temperature TPD peak is probably related to the presence of very weak silanol Bronsted sites due to defects in the crystalline structure of silicalite [38]. The higher temperature peak can be attributed to the presence of very small amount of tetrahedral aluminum atoms in the framework of silicalite which generate relatively strong zeolitic Brönsted acidity, similar to that of the isostructural ZSM-5 zeolite [39]. The total number of acid sites of the pure silicalite sample was determined about 0.11 mmol NH_3/g. As it can be seen from the TPD curves in Fig. 3b and the data in Table 2, the presence of bulk crystalline vanadia on the 4 wt.% V silicalite catalyst has a minor effect on the acidity of pure silicalite. It can thus be suggested that the monomeric vanadia species formed on the surface of mesoporous silicas are much more acidic compared to the bulk crystalline vanadia supported on the silicalite sample. This is further supported by the negligible acidity of the respective 4V-SiO_2 catalyst (Table 2) which contains also only bulk crystalline vanadia. The total number of acid sites of this catalyst is less than 0.01 mmoles/g NH_3 which is similar to that of the pure SiO_2 support.

3.2. Catalytic results in propane oxidative dehydrogenation

3.2.1. Effect of support type

In order to assess the catalytic performance of the vanadia catalysts supported on mesoporous, microporous and non-porous

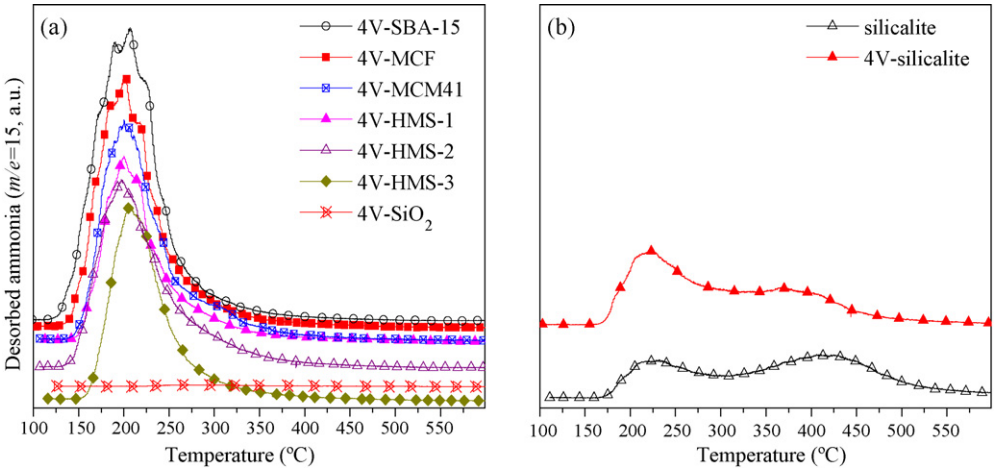

Fig. 3. TPD curves of (a) catalysts supported on different silicas with 4 wt.% V and (b) pure microporous silicalite and impregnated with 4 wt.% V.

silicas, the activity of the catalysts and the bare supports was investigated as a function of reaction temperature between 400 and 600 °C at W/F = 0.11 g s cm^{-3} using an equimolar propane and oxygen feed. The main products found were propene and CO/CO_2 which were formed mostly via the consecutive oxidation reactions of propene. Besides these products, ethylene, ethane and also oxygenates (acetaldehyde and acetic acid) were traced in small amounts. Apart from the silicalite, the other silica supports did not show any measurable activity even at the highest temperature used (600 °C). Silicalite showed ~8% conversion of propane at 600 °C. Furthermore, in the case of pure silicalite as well as the corresponding vanadia catalyst, the selectivity to ethylene and ethane was relatively high, implying that cracking reactions are taking place parallel to oxydehydrogenation. The selectivity to C_2 hydrocarbons (consisting mainly of ethylene) was about 7.5% at 25% propane conversion at 540 °C for the 4V-silicalite catalyst and 12.5% at 8% propane conversion for the pure silicalite support (at 600 °C). The cracking activity of the zeolite silicalite under relevant reaction conditions was also evidenced in the literature [5].

The propane conversion for the 4 wt.% V catalysts supported on mesoporous MCM-41, HMS, SBA-15, MCF, microporous zeolite silicalite and non-porous SiO_2 versus reaction temperature is shown in Fig. 4a. Except for the non-porous SiO_2, all the other supported vanadia catalysts show high propane conversions approaching 35–40% at reaction temperature of 550–575 °C. It is noteworthy that oxygen conversions attained under these conditions did not exceed 90%. Although the differences in activity observed for these catalysts in the whole temperature range tested were not so high, however, the following sequence of decreasing activity can be derived:

4V-HMS-1, 2, 3 ≈ 4V-MCM-41 ≈ 4V-silicalite
> 4V-SBA-15 ≈ 4V-MCF ≫ 4V-SiO_2

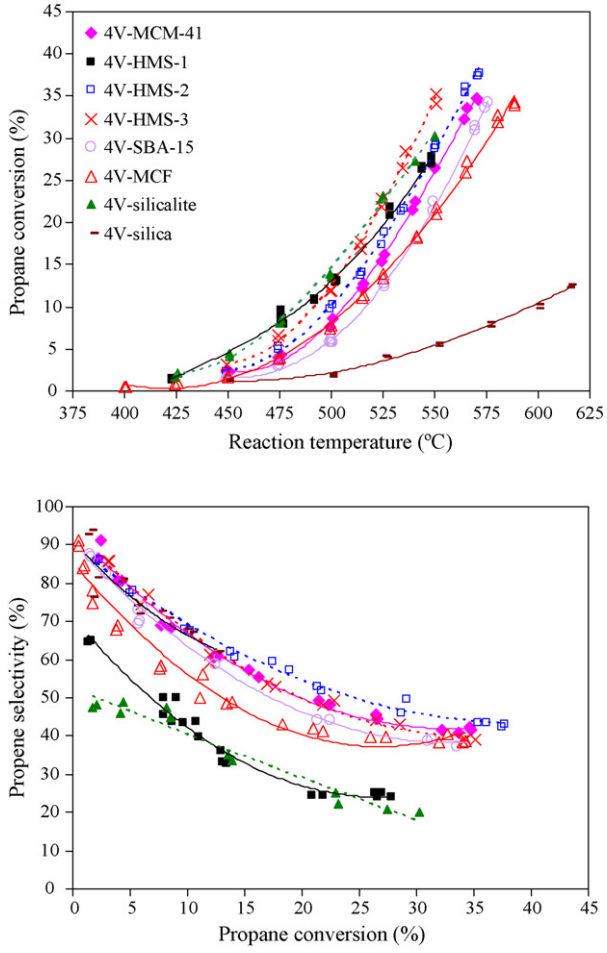

Fig. 4. (a) Propane conversion versus reaction temperature and (b) propene selectivity versus propane conversion for the 4 wt.% V supported catalysts (reaction conditions: F = 105 ml/min, W = 0.2 g, C_3H_8/O_2/He = 5/5/95).

The HMS and MCM-41 supported catalysts with relatively small mesopore size (2.3–3.3 nm) and the microporous silicalite supported catalyst exhibit higher activities compared to the SBA-15 and MCF supported catalysts that possess larger mesopore sizes (6.7 and 20 nm, respectively), probably due to the lower degree of vanadia dispersion in the latter group of catalysts. The lower vanadia dispersion in the SBA-15 and MCF supported catalysts is mainly attributed to the partial destruction of the mesopore structure and the respective loss of surface area during preparation of these catalysts, as explained above (see also Table 1). The observed marginally higher acidity of the SBA-15 and MCF supported catalysts (see Table 2) was not capable of inducing higher propane conversion compared to the HMS and MCM-41 supported catalysts. The high propane conversion for the silicalite based catalyst can be attributed to the presence of strong acid sites (as detected from NH_3-TPD), which favor not only the dehydrogenation reactions over vanadia sites but the cracking reactions as well on the silicalite support, as explained above. The very low surface area of the non-porous SiO_2 support resulted in poor dispersion of vanadium and the formation of bulk crystallline vanadia in the respective catalyst, thus leading to low activity in ODH of propane.

The selectivity to propene obtained at various temperatures as a function of conversion is presented in Fig. 4b. Worthy to notice that the products selectivity was independent of the reaction temperature as was evidenced by catalytic tests conducted at constant temperature and varying W/F (not shown for brevity). This series of tests confirmed that in propane ODH the selectivity to the products is entirely controlled by the degree of alkane conversion, at least for the types of catalysts studied in this work. Except for HMS-1 based catalysts, propene selectivities as high as 90% are achieved at initial steps of the reaction (low conversions) for all the catalysts supported on mesoporous materials. Selectivity of propene decreases with increasing propane conversion due to the consecutive oxidation of the olefin to a mixture of CO and CO_2. However, the extent of deep oxidation reactions is not so high since the selectivity to propene remains at relatively high levels (up to 40%) even for propane conversions of 30–40%. At isoconversion (10%) the sequence in decreasing selectivity is as follows: 4V-SiO_2 > 4V-HMS-2,3 ≈ 4V-MCM-41 ≈ 4V-SBA-15 ≈ 4V-MCF > 4V-HMS-1 ≈ 4V-silicalite

The low propene selectivity observed with the silicalite supported catalysts can be attributed to the extensive total oxidation pathways to CO_x (mainly CO_2) and to relatively enhanced cracking reaction routes on the silicalite support. On the other hand, the SiO_2 supported catalyst exhibited remarkably high propene selectivity, despite the presence of bulk V_2O_5 crystals. Blasco and Lopez Nieta [2] have noticed that the effect of the type of V^{5+} species is much stronger at high conversion levels where V_2O_5 crystals favor CO_x formation, while highly dispersed monomeric V^{5+} species ease the fast desorption of propene resulting in higher propene selectivities. Based on these findings, the high propene selectivity of the SiO_2 supported catalyst of our work can be attributed to the low propane conversion (up to ca. 12%, see Fig. 4b) without being significanlty affected by the type of V^{5+} species. In addition, the SiO_2 supported vanadia catalyst possesses negligible acidity (Table 2), which might be another reason for enhanced propene selectivity.

The effect on the activity and selectivity in ODH of propane of the textural properties and the pore size of the mesoporous supports can be evaluated by comparing the catalysts supported on hexagonal MCM-41 (pore diameter ~2.7–2.9 nm), wormhole-like HMS (pore diameter – HMS-1 ~ 2.2, HMS-2 ~ 2.7, HMS-3 ~ 3.2 nm), hexagonal SBA-15 (pore diameter ~6.5–6.7) and mesocellular foam MCF (pore diameter ~20 nm). The structure of MCM-41 and SBA-15 mesoporous silicas consists of tubular pores in hexagonal arrangement while the HMS and MCF silicas exhibit a 3-D disordered structure [20 and references therein]. In the case of HMS silicas, appropriate control of the synthesis conditions can lead to the formation of high textural porosity (voids between primary nanoparticles that consitute larger aggregate/particles) in addition to the framework mesoporosity with wormhole-like structure. Samples HMS-2 and HMS-3 exhibit this "double" porosity as is explained in Section 3.1. The presence of textural porosity in combination with the 3-D wormhole structure of the HMS type silicas can be beneficial for various reactions by enhancing diffusion of reactant and products towards and away from the metal active sites that reside on the surface of the pores [40]. From the catalytic results of the present work it can be suggested that there is no direct significant effect of the pore structure and size of the mesoporous supports and the respective vanadia catalysts on the activity and selectivity in the ODH of propane. There is, however, an indirect effect that is related with the partial breakdown of the structure of SBA-15 and MCF during preparation of the vanadia catalysts, which resulted in lower vanadia dispersion and also to the formation of non-skeletal silica phases that blocked access to the active VO_x phases inside the pores. Lower propane conversion compared to the MCM-41 and HMS supported catalysts were thus achieved with the SBA-15 and MCF catalysts. With regard to propene selectivity, the above effect was marginal since the majority of vanadia species in the SBA-15 and MCF supported catalysts was still present as isolated VO_x monomers.

3.2.2. Effect of V loading

The effect of vanadia loading (0.7–8 wt.% V) on the catalytic activity was also studied. For brevity, only the results obtained for the catalysts supported on mesoporous HMS-2 with different vanadia loadings (1.3–8 wt.%) are depicted in Fig. 5. Increase in the loading of V favors monotonically the propane conversion, implying an increase in the amount of active sites (Fig. 5a). As it concerns selectivity, catalysts with low V loadings up to 4 wt.% did not show any significant difference in selectivity while further increase to 8 wt.% was not beneficial (Fig. 5b). The relatively lower selectivity of the 8V-HMS-2 catalyst especially at high conversion levels implies higher rates of propene overoxidation. The higher acidity of this sample compared to the other HMS-2 supported catalysts with lower V loadings (Table 2) in combination with the presence of few V_2O_5 crystals (Fig. 1a) might be the reason for the decreased propene selectivity.

However, the above results cannot be used to gain an insight into the intrinsic rate of products formation. Turnover rates of propane consumption for the catalysts supported on high surface area mesoporous silicas with highly dispersed VO_x species were calculated based on the experimental results obtained at 500 °C for conversion values below ca. <10%. The pertinent results are plotted in Fig. 6 as a function of the VO_x surface density. As expected for the same VO_x density, the differences in TOFs are marginal among the mesoporous supported catalysts. However, a relatively strong correlation of TOF with the VO_x density is evident. With reference to the observed drop in TOF (activity for propane conversion *per* V) versus n_s, one could state that on the basis of stable site reactivity, this trend should concur with the trend in the

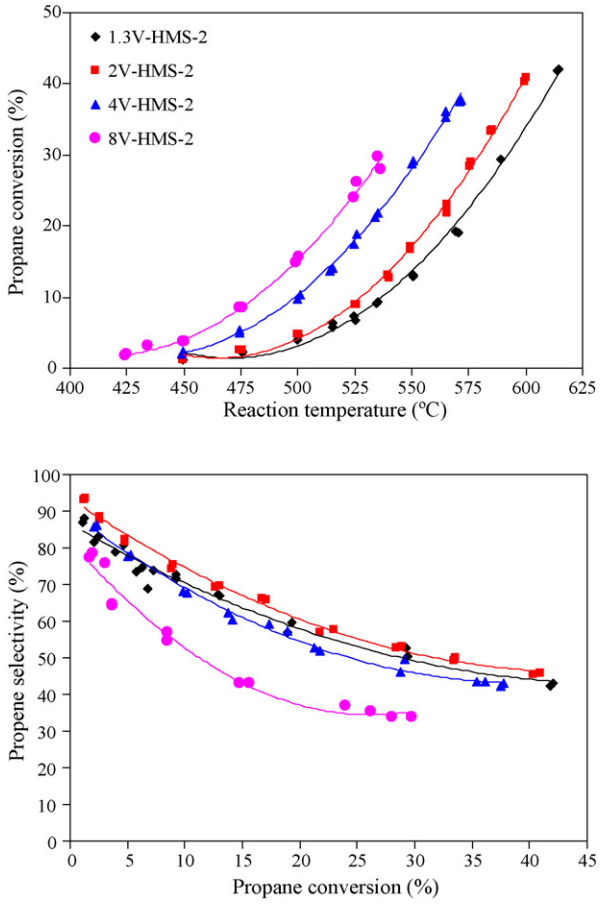

Fig. 5. (a) Propane conversion versus reaction temperature and (b) propene selectivity versus propane conversion for vanadia catalysts supported on HMS-2 mesoporous silica with different V loadings (reaction conditions: F = 105 ml/min, W = 0.2 g, $C_3H_8/O_2/He$ = 5/5/95).

number of active sites *per* V. Thus, the V=O site can be excluded from being active, since there is always one V=O *per* V in each isolated $(Si–O–)_3V=O$ unit (for coverage below monolayer) and the protruding nature of the V=O sites would assure their availability and would therefore result in a constant TOF versus n_s trend. To the contrary, although the number of anchoring V–O–Si sites is also stable (there are three such sites *per* V) it is very probable that such sites become increasingly inaccessible and unavailable for C–H

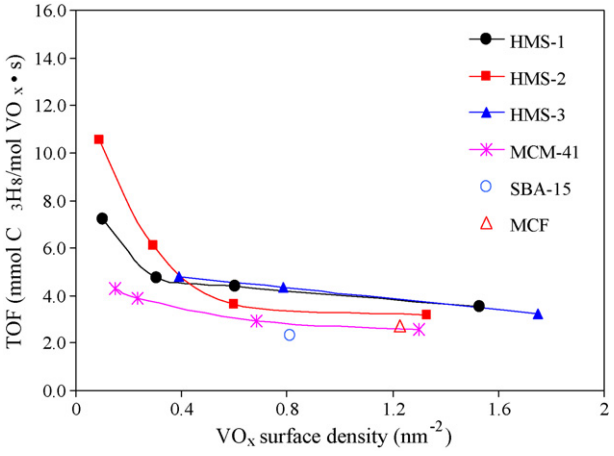

Fig. 6. TOF of propane as a function of VO_x surface density (T = 500 °C).

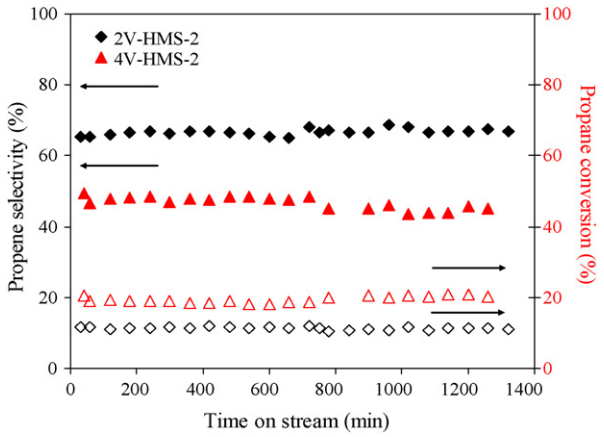

Fig. 7. Propane conversion and propene selectivity in ODH of propane at 525 °C for vanadia catalysts supported on HMS-2 with 2 and 4 wt.% V for long reaction time.

bond activation as a result of increasing congestion of monomeric VO_4 units, as those units are bunched around each other with increasing n_s, below monolayer. This would result in a decrease of the propane TOF versus n_s, as seen in Fig. 6. Thus, the V–O–Si sites could be designated as the sites for the activation of propane. In addition, the TOF values for propene formation follow the same trend as with propane TOF since the data in Fig. 6 refer to low propane conversion (below 10%), at which the measured selectivity to propene was higher than ca. 80% for all catalysts supported on mesoporous silicas. Finally, the changes in TOF cannot be ascribed to alterations in bond strength within the V–O–Si anchoring bridges; such alterations in bond strength (should they have been occurred) would result in complementary changes in the V=O bond strength. However, the position of the V=O band is not affected by increase in V loading (see e.g. Fig. 1a)

Evaluating the overall catalytic performance in propane ODH in terms of propene yield, based on the activity/selectivity results (Figs. 4 and 5) we propose as the most promising catalytic samples those supported on HMS-2 mesoporous silica which possess medium mesopore sizes of 2.7–2.8 nm (compared to the other mesoporous silicas) and additional textural porosity as high as 0.6 cm^3/g. High propene yields about 16–19% at 575–600 °C for low vanadium loadings (2–4 wt.%) were obtained, ranking these catalysts among the best performing vanadia catalysts according to a recent review [10].

3.2.3. Stability of HMS-2 supported catalysts

Apart from the activity and selectivity, stability is also of paramount importance in propane ODH. Two of the most promising catalysts, the 2 and 4 wt.% V supported on HMS-2 (2V-HMS-2 and 4V-HMS-2 respectively), were tested in propane ODH at 525 °C for 24 h time on stream. Propane conversion and propene selectivity as a function of TOS for both materials are compiled in Fig. 7. The unchanged profiles of propane conversion and propene selectivity demonstrate the superior stability of the mesoporous supported vanadia catalysts, implying that the mesoporous supports retain their structure and the high vanadia dispersion under reaction conditions for extended period of time.

4. Conclusions

Vanadia catalysts supported on MCM-41 and HMS mesoporous silicas showed the best catalytic performance compared to other mesoporous silicas (SBA-15, MCF), mircroporous silicalite and non-porous SiO_2 supported vanadia catalysts in the ODH of propane. Highly dispersed monomeric VO_x species can be achieved on these high surface area silicas even for V loadings of 8 wt.% thus leading to very active catalysts. However, the highest propene yields (16–19%) were accomplished at relatively low V loadings (2–4 wt.% V). The differences in propane TOFs were marginal among the mesoporous supported catalysts implying that the mesopore structure and size has a limited direct effect on catalyst's intrinsic activity. However, a superior performance of the catalyst supported on HMS mesoporous silica with 3-D wormhole pore structure and medium mesopore size (2.7–2.8 nm) in combination with high textural porosity (interparticle voids) could be identified. The slightly lower activity of the catalysts supported on SBA-15 and MCF mesoporous silicas was attributed to the partial destruction of the mesopore structure during preparation of the catalysts, thus leading to relatively lower vanadia dispersion and also to the formation of non-skeletal silica phases that blocked access to the active VO_x phases inside the pores. The presence of strong acid sites on the surface of microporous zeolite silicalite induced high propane conversion with the respective supported vanadia catalysts but at the same time gave rise to direct oxidation of propane towards CO_2 and cracking reactions. In addition, the presence of bulk crystalline vanadia on these catalysts favored the consecutive overoxidation reactions of propene at relatively high conversions/temperatures. On the other hand, the non-porous SiO_2 supported catalysts were not active mainly due to their low surface area and consequently the poor vanadia dispersion but were quite selective towards propene since they operated at low conversions even for relatively high reaction temperatures.

Acknowledgements

This work was co-financed by E.U.–European Social Fund and the Greek Ministry of Development-GSRT through the programme EPAN-PENED2003.

References

[1] G. Centi, F. Cavani, F. Trifirò, Selective Oxidation by Heterogeneous Catalysis, Fundamental and Applied Catalysis, Kluwer Academic, New York, 2001, p. 204.
[2] T. Blasco, J.M. Lopez Nieto, Appl. Catal. A 157 (1997) 117.
[3] E.A. Mamedov, V. Cortes-Corberan, Appl. Catal. A 127 (1995) 1.
[4] M. Machli, E. Heracleous, A.A. Lemonidou, Appl. Catal. 236 (2002) 23.
[5] G. Centi, F. Trifiro, Appl. Catal. A 143 (1996) 3.
[6] A. Christodoulakis, M. Machli, A.A. Lemonidou, S. Boghosian, J. Catal. 222 (2004) 293.
[7] K. Routray, K.R.S.K. Reddy, G. Deo, Appl. Catal. A 265 (2004) 103.
[8] A. Khodakov, B. Olthof, A.T. Bell, E. Iglesia, J. Catal. 181 (1999) 205.
[9] E.V. Kondratenko, M. Cherian, M. Baerns, Catal. Today 112 (2006) 60.
[10] F. Cavani, N. Ballarini, A. Cericola, Catal. Today 127 (2007) 113.
[11] E.V. Kondratenko, M. Cherian, M. Baerns, D. Su, R. Schlögl, X. Wang, I.E. Wachs, J. Catal. 234 (2005) 131.
[12] M.L. Pena, A. Dejoz, V. Formés, F. Rey, M.I. Vásquez, J.M. López Nieto, Appl. Catal. A 209 (2001) 155.
[13] Y. Wang, Q. Zhang, Y. Ohishi, T. Shishido, K. Takehira, Catal. Lett. 72 (2001) 215.
[14] O.V. Buyevskaya, A. Brückner, E.V. Kondratenko, D. Wolf, M. Baerns, Catal. Today 67 (2001) 369.
[15] R. Zhou, Y. Cao, S. Yan, J. Deng, Y. Liao, B. Hong, Catal. Lett. 75 (2001) 107.
[16] P. Knotek, L. Čapek, R. Bulánek, J. Adam, Top. Catal. 45 (2007) 51.
[17] Y.-M. Liu, Y. Cao, N. Yi, W.-L. Feng, W.-L. Dai, S.-R. Yan, H.-Y. He, K.-N. Fan, J. Catal. 224 (2004) 417.
[18] F. Ying, J. Li, C. Huang, W. Weng, H. Wan, Catal. Lett. 115 (2007) 137.
[19] Y.-M. Liu, W.-L. Feng, T.-C. Li, H.-Y. He, W.-L. Dai, W. Huang, Y. Cao, K.-N. Fan, J. Catal. 239 (2006) 125.
[20] S.A. Karakoulia, K.S. Triantafyllidis, A.A. Lemonidou, Micropor. Mesopor. Mater. 110 (2008) 157.
[21] J. Due-Hansen, S. Boghosian, A. Kustov, P. Fristrup, G. Tsilomelekis, K. Stahl, C. Hviid Christensen, R. Fehrmann, J. Catal. 251 (2007) 459.
[22] H. Tian, E.I. Ross, I.E. Wachs, J. Phys. Chem. B 110 (2006) 9593.
[23] D.E. Keller, T. Visser, F. Soulimani, D.K. Koningsberger, B.M. Weckhuysen, Vibr. Spectr. 43 (2007) 140.
[24] X. Gao, S.R. Bare, B.M. Weckhuysen, I.E. Wachs, J. Phys. Chem. B 102 (1998) 10842.
[25] I.E. Wachs, Catal. Today 27 (1996) 437.
[26] G. Deo, I.E. Wachs, J. Catal. 146 (1994) 323.
[27] S. Xie, E. Iglesia, A.T. Bell, Langmuir 16 (2000) 7162.
[28] C. Hess, G. Tzolova-Müller, R. Herbert, J. Phys. Chem. C 111 (2007) 9471.
[29] G. Deo, I.E. Wachs, J. Phys. Chem. 95 (1991) 5889.

[30] H. Berndt, A. Martin, A. Brücker, E. Schreier, D. Müller, H. Kosslick, G.-U. Wolf, B. Lücke, J. Catal. 191 (2000).
[31] B. Solsona, T. Blasco, J.M. López Nieto, M.L. Pena, F. Rey, A. Vidal-Moya, J. Catal. 203 (2001) 243.
[32] C.-B. Wang, R.G. Herman, C. Shi, Q. Sun, J.E. Roberts, Appl. Catal. A 247 (2003) 321.
[33] G. Grubert, J. Rathouský, G. Schulz-Ekloff, M. Wark, A. Zukal, Microporous Mesoporous Mater. 22 (1998) 225.
[34] J. Santamaría-González, J. Luque-Zambrana, J. Mérida-Robles, P. Maireles-Torres, E. Rodríguez-Castellón, A. Jiménez-López, Catal. Lett. 68 (2000) 67.
[35] W. Liu, S.Y. Lai, H. Dai, S. Wang, H. Sun, C.T. Au, Catal. Lett. 113 (2007) 147.
[36] Q. Zhang, Y. Wang, Y. Ohishi, T. Shishido, K. Takehira, J. Catal. 202 (2001) 308.
[37] Y.-M. Liu, Y. Cao, K.-K. Zhu, S.-R. Yan, W.-L. Dai, H.-Y. He, K.-N. Fan, Chem. Comm. (2002) 2832.
[38] G. Centi, S. Perathoner, F. Trifiró, A. Aboukais, C.F. Aissi, M. Guelton, J. Phys. Chem. 96 (1992) 2617.
[39] K.S. Triantafyllidis, L. Nalbandian, P.N. Trikalitis, A.K. Ladavos, T. Mavromoustakos, C.P. Nicolaides, Microporous Mesoporous Mater. 75 (2004) 89.
[40] A.P. Fotopoulos, K.S. Triantafyllidis, Catal. Today 127 (2007) 148.